Electrochemistry Communications 92 (2018) 9–13

Contents lists available at ScienceDirect

Electrochemistry Communications

journal homepage: www.elsevier.com/locate/elecom

Formation of a thin-layer of nickel hydroxide on nickel phosphide nanopillars for hydrogen evolution

Kun Xiong[a,*], Liping Huang[a], Yuan Gao[a], Haidong Zhang[a], Yue Zhuo[a], Huizhen Shen[a], Yao Wang[b], Lishan Peng[b], Zidong Wei[b,*]

[a] Chongqing Key Laboratory of Catalysis & Environmental New Materials, Engineering Research Center for Waste Oil Recovery Technology and Equipment of Ministry of Education, Chongqing Technology and Business University, Chongqing 400067, China
[b] Chongqing Key Laboratory of Chemical Process for Clean Energy and Resource Utilization, School of Chemistry and Chemical Engineering, Chongqing University, Chongqing 400044, China

ARTICLE INFO

Keywords:
Nickel hydroxide
Nickel phosphide
Etching
Hydrogen evolution reaction

ABSTRACT

A thin-layer of $Ni(OH)_2$ was *in situ* formed on the surface of Ni_2P nanopillars ($Ni(OH)_2$@Ni_2P/E-NF) *via* a facile hydrothermal treatment in H_2O. $Ni(OH)_2$@Ni_2P/E-NF exhibits superior activity for the hydrogen evolution reaction with an overpotential of only 43 mV to achieve 10 mA cm^{-2} and a good durability during the long-term operation in an alkaline medium. The excellent performance of $Ni(OH)_2$@Ni_2P/E-NF is likely ascribed to the strong interfacial coupling of $Ni(OH)_2$ and Ni_2P, which promotes the dissociation of water and concomitantly converts hydrogen intermediates (H_{ad}) to H_2.

1. Introduction

Hydrogen is a potential energy carrier due to its high energy density and environmentally friendly advantages [1]. Water electrolysis is one of the most promising technologies to produce high-purity hydrogen. The typical catalyst for the hydrogen evolution reaction (HER) is Pt, whose scarcity and high cost extremely hamper its wide-scale applications. Thus, many research efforts have been devoted to exploiting non-Pt catalysts, such as transition metal carbides [2,3], sulfides [4,5], nitrides [6,7], and phosphides [8–16].

Transition metal phosphides (TMPs) are considered potential Pt alternatives since they can present high HER activity. However, their intrinsic activities are still inferior to those of precious metal catalysts because of insufficient cleavage of the HO-H bond in H_2O. Hence, promoting the water dissociation process on TMPs is essential to further improve their HER activity. Some studies have demonstrated that introducing ($Ni(OH)_2$) to the surface of metal catalysts as a water dissociation promoter would likely accelerate alkaline HER processes [17–19].

Herein, we developed a method to engineer the interface of Ni$(OH)_2$@Ni_2P through a phosphorization process and hydrothermal treatment in pure water. In the HER catalysed by $Ni(OH)_2$@Ni_2P/E-NF, Ni_2P acts as the main reactive centres, while $Ni(OH)_2$ is expected to be the secondary active sites for accelerating the dissociation of water to improve the electrocatalytic activity.

2. Experimental

2.1. Materials synthesis

First, 1.89 g of oxalic acid (Adamas) was dissolved in the mixed solution of 15 mL of ethanol and 15 mL of deionized water. Then, the solution was transferred to a 50 mL autoclave with a piece of Ni Foam (NF, 50.0 mm × 10.0 mm). The autoclave was treated at 100 °C for 5 h to etch the NF. Afterward, the etched NF (E-NF) and NaH_2PO_2 were placed in alumina boats and heated at 350 °C for 2 h in an Ar atmosphere to form Ni_2P/E-NF. Finally, Ni_2P/E-NF was heated at 180 °C for 10 h in 30 mL of deionized water to achieve the spontaneous growth of a thin-layer of $Ni(OH)_2$ on Ni_2P/E-NF. The loading of catalyst on NF is 1.26 mg cm^{-2}. For comparison, $Ni(OH)_2$@Ni_2P/E-NF-x (x = 5, 10, and 24 h, respectively) with different content of $Ni(OH)_2$ were prepared by regulating the hydrothermal time.

2.2. Characterizations and electrochemical measurements

X-ray diffraction (XRD) measurements were taken on a Shimadzu XRD-6000 instrument with Cu−K radiation (λ = 1.54184 Å). Scanning electron microscope (SEM) images were obtained on a JSM-7800 field-emission scanning electron microscope, while transmission electron microscope (TEM) images were obtained on an FEI Tecnai F20 X-Twin microscope. Electrochemical measurements were conducted in a three-

* Corresponding authors.
E-mail addresses: kunxiong@email.ctbu.edu.cn (K. Xiong), zdwei@cqu.edu.cn (Z. Wei).

https://doi.org/10.1016/j.elecom.2018.05.016
Received 5 May 2018; Received in revised form 11 May 2018; Accepted 11 May 2018
Available online 12 May 2018

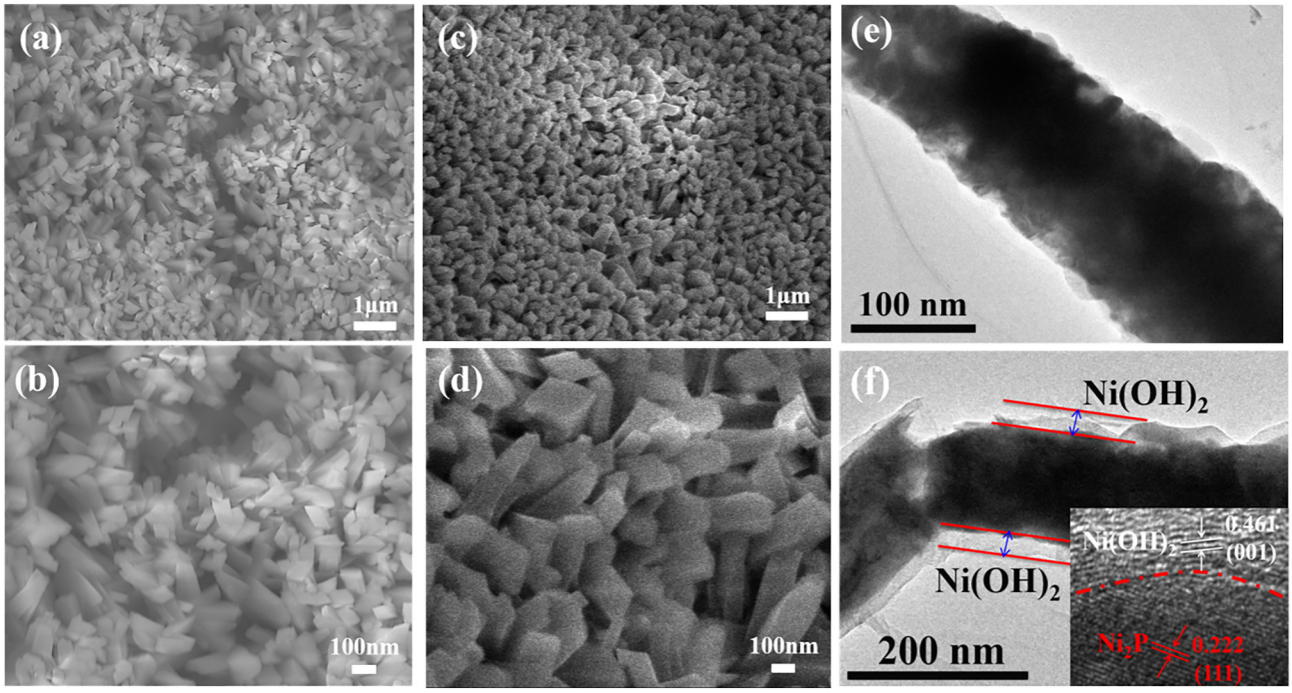

Fig. 1. FE-SEM images of (a and b) Ni_2P/E-NF; (c and d) $Ni(OH)_2$@Ni_2P/E-NF; TEM images of (e) Ni_2P/E-NF and (f) $Ni(OH)_2$@Ni_2P/E-NF (the inset is the high-magnification image).

electrode cell system with an electrochemical workstation (Autolab electrochemical analyzer, PGSTAT302 N, Metrohm). A graphite sheet was used as the counter electrode, and a mercuric oxide electrode (Hg/HgO) was employed as the reference electrode. The HER activity of the catalysts was investigated in 1.0 M KOH electrolyte at a rate of 1 mV s^{-1}. Electrochemical active surface areas (ECSAs) of the catalysts were determined by the equation: ECSA = $R_f \times S$, where S was 1 cm^2 and the R_f was determined by $R_f = C_{dl}/60\ \mu F\ cm^{-2}$ based on the double-layer capacitance (C_{dl}) of a smooth oxide surface (60 μF cm^{-2}) [20,21]. Electrochemical impedance spectroscopy (EIS) measurements were taken at an overpotential of 50 mV in the frequency range of 100 kHz to 0.1 Hz.

3. Results and discussion

It can be seen from Fig. 1 that the surface of NF is uniformly covered with Ni_2P nanopillars after etching the surface of NF and phosphorization. That is, oxalic acid as a weak acid can etch the surface of NF to form a nanopillar structure. This unique structure increases the surface area, and thus helps to maximize the number of exposed active sites. After being subjected to the hydrothermal treatment in pure water, the surface of Ni_2P/E-NF became rough with the formation of a thin-layer of $Ni(OH)_2$, which is clearly proved by the TEM images of $Ni(OH)_2$ with a discontinuous lattice fringe. The growth of $Ni(OH)_2$ is attributed to the weak oxidation of nickel in pure H_2O during the hydrothermal treatment [22]:

$$Ni + nH_2O \rightarrow [Ni(H_2O)n]^{2+} + 2e^-$$

$$O_2 + 2H_2O + 4e^- \rightarrow 4OH^-$$

$$[Ni(H_2O)n]^{2+} + 2OH^- \rightarrow Ni(OH)_2 + n\ H_2O$$

The XRD patterns of catalysts are shown in Fig. 2a. Ni_2P/E-NF shows diffraction peaks at 40.8°, 44.6°, 47.3°, 54.2°, 54.9°, and 74.7° indexed to Ni_2P (JCPDS No. 03-0953), and the other peaks arise from Ni substrate (JCPDS No. 04-0850). After the hydrothermal treatment for 10 h, the intensity of Ni_2P diffraction peaks decreases, and no peaks of $Ni(OH)_2$ are detected on $Ni(OH)_2$@Ni_2P/E-NF-10 h because of its low content and poor crystal structure. When the hydrothermal time is extended to 24 h, the broad peaks at 19.2°, 33.1°, 38.5°, and 59.0° observed for $Ni(OH)_2$@Ni_2P/E-NF-24 h confirms the presence of $Ni(OH)_2$ (JCPDS No. 14-0117). In the Ni 2p XPS spectrum (Fig. 2b), the peak at 852.2 eV is assigned to low-valence $Ni^{\delta+}$ ($0 \le \delta < 2$), suggesting the formation of phosphides [23]. The peaks at 855.8 and 873.5 eV with two satellite peaks are characteristic of Ni^{2+} [22]. Fig. 2c shows two peaks at 129.9 and 132.4 eV corresponding to phosphides and oxidized phosphorus species arising from superficial oxidation [24]. The O 1 s spectrum (Fig. 2d) reveals the presence of O^{2-} at 529.5 eV, OH^- at 531.3 eV, and physi- and chemisorbed water at 533.2 eV. These results provide another piece of evidence to support the formation of $Ni(OH)_2$ on Ni_2P/E-NF.

The HER activity of catalysts was evaluated in 1.0 M KOH by using a three-electrode system (Fig. 3a). As expected, 20 wt% Pt/C exhibits an extremely high activity toward HER, while NF shows the poorest HER activity. Note that $Ni(OH)_2$@Ni_2P/E-NF-10 h shows a greatly enhanced HER activity compared to that of Ni_2P/E-NF without $Ni(OH)_2$. Furthermore, it needs an overpotential of only 43 mV to achieve 10 mA cm^{-2}, which is much lower than that of Ni_2P/E-NF ($\eta_{10\ mA\ cm^{-2}}$ = 90 mV) and other Ni phosphides reported in the literature, such as Ni_2P/Ti ($\eta_{20\ mA\ cm^{-2}}$ = 138 mV) [8], porous Ni_2P nanoparticle ($\eta_{20\ mA\ cm^{-2}}$ = 250 mV) [13], Ni_2P/Ni/NF ($\eta_{10\ mA\ cm^{-2}}$ = 98 mV) [14], Ni_2P polyhedrons ($\eta_{10\ mA\ cm^{-2}}$ = 146 mV) [15], and Mo-Ni_2P NWs/NF ($\eta_{10\ mA\ cm^{-2}}$ = 67 mV) [16]. The excellent performance of $Ni(OH)_2$@Ni_2P/NF-10 h could be ascribed to the interfacial coupling of $Ni(OH)_2$ and Ni_2P, in which $Ni(OH)_2$ promotes the dissociation of water and concomitantly generates more hydrogen intermediates (H_{ad}) on the nearby Ni_2P to form H_2. To obtain the optimized $Ni(OH)_2$ on Ni_2P, three $Ni(OH)_2$@Ni_2P/E-NF-x (x = 5, 10, and 24 h, respectively) with different content of $Ni(OH)_2$ were prepared by regulating the hydrothermal time. Table 1 shows that the atomic concentration of Ni and O increases with the increment of reaction time, whereas the P exhibits an opposite trend. This implies the gradual increase of $Ni(OH)_2$ on the surface of Ni_2P. For $Ni(OH)_2$@Ni_2P/E-NF-5 h, because of little $Ni(OH)_2$ formed on the surface of Ni_2P, it is rational to observe that its activity is similar to that of Ni_2P/E-NF. When the atomic concentration of Ni and